INTERNATIONAL JOURNAL OF CLIMATOLOGY
Int. J. Climatol. (2016)
Published online in Wiley Online Library
(wileyonlinelibrary.com) DOI: 10.1002/joc.4894

Royal Meteorological Society

A probabilistic approach for attributing temperature changes to synoptic type frequency

Irene B. Nilsen,* James H. Stagge and Lena M. Tallaksen
Department of Geosciences, University of Oslo, Norway

ABSTRACT: To understand the cause of regional temperature change, it is common to separate the temperature change signal into changes in atmospheric synoptic circulation and other factors, so-called within-type changes. In this study, we suggest a novel probabilistic approach that allows detection of months and regions where temperature changes can mainly be attributed to changes in synoptic circulation and where within-type changes also play a role. By combining resampling with a Monte Carlo test, we assess the likelihood that the observed warming can be explained by synoptic circulation changes alone. This method is applicable for any variable, and in any region of the world. We applied it to an example case using gridded WATCH Forcing Data ERA-Interim (WFDEI) temperature data and synoptic types derived from the SynopVis Grosswetterlagen catalogue (1981–2010). For this European example, the most widespread warming was found in summer, with up to 60% of the land area experiencing significant warming during August, notably in Eastern and Northern Europe. In spring and autumn, this area was reduced to 10–30%. In December and January, only about 5% of the land area experienced significant warming, most pronounced in northern Scandinavia. The probabilistic approach revealed that changes in synoptic circulation could not account for all the observed (WFDEI) warming, with the exception of regions in southeastern Europe in February and Western Europe in May. Significant warming in other months and regions, such as the large-scale warming in April, June, July, August, and November, must also be caused by other factors. Within-type changes were confirmed for the Black Sea region in November, where the magnitude of a widespread temperature trend was strongest. This European example contributes to an improved understanding of the causes of recent temperature change by assessing the relative role of synoptic circulation changes and within-type changes on regional-scale warming.

KEY WORDS temperature; trend detection; trend attribution; atmospheric circulation; within-type changes; probabilistic approach; dynamic causes; thermodynamic causes

Received 25 February 2016; Revised 25 July 2016; Accepted 22 August 2016

1. Introduction

"From the deep oceans to the top of the troposphere, the evidence of warmer air and oceans, of melting ice and rising seas all points unequivocally to one thing: the world has warmed since the late 19th century" (Hartmann *et al.*, 2013). Globally, the warming has been most pronounced after 1970 (Hartmann *et al.*, 2013), and Europe has warmed faster than the global mean land trend (Christensen *et al.*, 2013). Annual land temperatures averaged over Europe were 1.5 °C higher in the 2005–2014 average compared with the 1850–1899 average (EEA, 2015). Strong warming trends have been reported for the period 1976–2006 in the Mediterranean region during summer (up to 0.3 °C decade^{-1}) and in Scandinavia during winter (up to 0.6 °C decade^{-1}) (EEA, 2008). The location and magnitude of the most pronounced warming vary with region, time of the year, and period chosen however. For instance, Jones *et al.* (2012) found that the European winter warmed fastest when analysed over a 150-year period (1861–2010), whereas spring warmed fastest when the same data were analysed over the shorter, most recent 110- and 32-year periods. Cooling is also seen for some seasons and regions during recent decades, particularly during autumn in Central and Eastern Europe [1976–1999; Klein Tank *et al*. (2005) and 1961–1998; Cahynová and Huth (2009)]. These studies are some examples of the wide amount of evidence of observed changes in temperature in Europe. To understand the nature of these changes, we must study whether their driving mechanisms can mainly be related to synoptic circulation changes or whether other factors play a role as well.

Detection of change in a climate variable such as temperature does not say anything about the underlying cause. Attribution of climate change is "the process of evaluating the relative contributions of multiple causal factors to a change or event with an assignment of statistical confidence" (Bindoff *et al.*, 2013). The physics of long-term global temperature trends and its link to variations in greenhouse gases are well studied and understood; however, for shorter time scales and smaller regions, the detailed mechanisms of such a change are not completely understood (Vautard and Yiou, 2009). Warming signals at this scale may manifest as a change in atmospheric

* Correspondence to: I. B. Nilsen, Department of Geosciences, University of Oslo, P.O. Box 1047, Blindern 0316, Oslo, Norway. E-mail: i.b.nilsen@geo.uio.no

© 2016 Royal Meteorological Society

circulation, favouring more frequent warm circulation patterns (Corti *et al.*, 1999). For example, increasing temperatures due to an increase in greenhouse gases can alter the position and strength of the polar jet stream (e.g. Cohen *et al.*, 2014). Saffioti *et al.* (2015) studied the mid-latitude Northern Hemisphere warming hiatus in the period 1998–2012, and found that circulation changes contributed to winter warming in the period before 2000, but led to cooling in the winters after 2000. Early weather prediction, prior to the advent of numerical weather prediction models, relied on such relationships between the local climate and synoptic circulation, and assumed that local climate trends could be explained by changes in circulation alone (Yarnal, 1993).

Warming may alternatively be entirely independent of circulation, occurring as a general increase in surface temperature. Cases when the circulation cannot explain all the observed temperature changes are widely documented (Barry and Perry, 1969; Beck *et al.*, 2007; Cahynová and Huth, 2009; Jones and Lister, 2009; Küttel *et al.*, 2011; Fleig *et al.*, 2015). The process causing warming in the absence of synoptic type (ST) frequency changes is called 'within-type changes' (Barry and Perry, 1969), defined as a change in the properties of the air masses over time (Beck *et al.*, 2007). For temperature, this means warming or cooling. Since then, efforts have been made to separate the causes of recent warming into these two components: changes in large-scale circulation (circulation changes) and other factors (within-type changes).

The importance of circulation changes relative to within-type changes varies depending on the region and time of year. Circulation changes have been found to relate closely to observed warming in Europe, especially in winter, but cannot explain all the observed warming (e.g. Corti *et al.*, 1999; Vautard and Yiou, 2009; Hoy *et al.*, 2013b; Fleig *et al.*, 2015). Beck *et al.* (2007) analysed monthly temperatures for Central Europe for the period 1780–1995 and found that circulation changes influenced trends in spring, winter, and autumn, but the importance of circulation changes varied over multidecadal time scales. Similarly, Cahynová and Huth (2010) found circulation changes in seasons other than winter to be of minor importance for temperature at stations in the Czech Republic (1961–1998). The above-mentioned studies all conclude that within-type changes explained a large part of the historical temperature trends, especially in summer for Central Europe (Beck *et al.*, 2007), though they differ slightly in their findings for other regions. Küttel *et al.* (2011) analysed gridded temperature and precipitation time series for all of Europe and concluded that within-type changes were also important for temperature changes in winter, especially in Eastern Europe and Scandinavia. One of the reasons for the different response in winter and summer is that winter weather is dominated by advective, large-scale processes, whereas summer weather is dominated by radiative, small-scale processes.

Most of the previous studies analysed changes on the seasonal scale using 3-month averages. Fleig *et al.* (2015) argued that an analysis of climate trends and their large-scale climatological causes should rather be performed at the monthly time scale. This is because some patterns of synoptic circulation occur more often in specific months (Hoy *et al.*, 2013a; Vrac *et al.*, 2014) and changes in circulation frequency may be masked when averaged over several months. Further, short-term trend patterns, such as responses related to changes in snow cover or greening, may be revealed at a monthly, but not a seasonal, time scale. Fleig *et al.* (2015) found that within-type changes played a role in April (Western Europe), July (Southern Europe), and September (Southern Europe). Their study was based on the WATCH Forcing Dataset for Europe covering the period 1963–2001.

Various methods have been applied to link circulation to local climate. One such approach is to classify climate variables into distinct STs (e.g. Yarnal, 1993). Such classifications group days having the same pattern of airflow and pressure systems into the same ST. An ST is a single nominal value characterizing the large-scale state of the atmosphere over a given domain and day. Circulation classifications are most commonly calculated from pressure fields over the domain of interest explaining the synoptic system in detail. One of the most widely used classifications is the Hess-Brezowsky Grosswetterlagen (Werner and Gerstengarbe, 2010), which was originally developed for Germany by Baur *et al.* (1944). It was further refined by Hess and Brezowsky (1977), and has proved valid for a larger part of Europe (James, 2007). Automated methods have recently improved classification of pressure fields, and James (2007) developed an objective version of the Hess-Brezowsky Grosswetterlagen covering the period 1871–2012, named the Objective-Grosswetterlagen. It is referred to as 'objective' because it uses STs inherited from the Hess-Brezowsky Grosswetterlagen, but allocation into STs is automated (James, 2007). The Objective-Grosswetterlagen was refined into SynopVis Grosswetterlagen (SVG) and provides several improvements including the use of additional climate variables in the ST classification (see Section 2.1 for further details).

The influence of circulation on temperature trends can be analysed by the method of hypothetical trends, introduced by Leathers and Ellis (1996), who studied STs causing extreme snowfall across the Great Lakes (United States). Using this method, a new hypothetical time series is constructed by replacing all observations with the long-term mean daily temperature for the given month and ST. The ratio of the hypothetical trend to the observed trend, called the trend ratio, was introduced by Cahynová and Huth (2009) as a way to estimate the relative influence of circulation changes on the observed warming. However, the trend ratio has some limitations as discussed by Fleig *et al.* (2015). This includes the trend ratio's inability to capture changes when both circulation changes and within-type changes play a role, but in opposite directions (i.e. representing warming and cooling, respectively), and when the observed trend is near zero. Division by a very low value will result in an unrealistically high trend ratio, thus suggesting that circulation changes play a dominating role, but

© 2016 Royal Meteorological Society

is in fact a calculation artefact. Cahynová and Huth (2009) and Fleig *et al.* (2015) avoided this problem by reporting trend ratios only for significant trends, whereas Hoy *et al.* (2013b) introduced an arbitrary cut-off at ±0.5 °C in their plots. This study builds on the work of Fleig *et al.* (2015), who used hypothetical trends and trend ratios following Cahynová and Huth (2009) to quantify the relative contribution of circulation changes on observed temperature and precipitation trends in Europe. To avoid the limitations of the trend ratio approach, there is a need for a method that evaluates the statistical significance of synoptic circulation changes on observed climate trends.

The aim of this study is to introduce a probabilistic expansion of the method of hypothetical trends that allows detection of months and regions where temperature changes can be attributed to changes in ST frequency alone. This novel method is hereafter referred to as the probabilistic approach, and the resulting set of hypothetical trends is referred to as synoptic-circulation-induced trends. The probabilistic approach provides a statistical test of whether the observed trends can be explained by changes in synoptic circulation alone, or not. This is accomplished by estimating the likelihood that the observed trend can be captured by the distribution of synoptic-circulation-induced trends using a Monte Carlo test. To demonstrate the method, we analyse recent temperature trends in Europe based on the WATCH Forcing Data ERA-Interim (WFDEI) data set for the period 1981–2010 and assess whether WFDEI temperature trends can be attributed to changes in ST frequency alone. The SVG is used to derive the distribution of synoptic-circulation-induced trends, derived by repeated resampling. The importance of within-type changes for months and regions with unique responses is confirmed by analysing whether groups of warm, medium, and cool STs have become warmer or cooler over time. This study provides a flexible statistical test that can be applied in any region of the world and for other climate variables to attribute the relative importance of synoptic changes on climate trends. The European example analysis also provides an important contribution towards an improved understanding of the role of the two main components of large-scale temperature change, i.e. synoptic circulation changes and within-type changes, for Europe specifically and points out regions and seasons that require additional focused study.

2. Data

2.1. Synoptic circulation classification, SVG

A daily catalogue of STs for Europe, the SVG (provided by P. James, 2013; personal communication) was selected for this study. The SVG is an updated version of the Objective-Grosswetterlagen catalogue (James, 2007), with some methodological improvements described in detail by Hoy *et al.* (2013a) and summarized in Fleig *et al.* (2015) and Wapler and James (2015). These improvements include using additional input variables and improving the climate mean composites used for correlation so they span the most common synoptic conditions more effectively (Hoy *et al.*, 2013a). SVG is derived from mean sea level pressure, precipitable water, 500–1000 hPa thickness, and 500 hPa geopotential height. All variables are taken from the Twentieth Century Global Reanalysis (Compo *et al.*, 2011) and supplemented by NCEP/NCAR reanalyses (Kalnay *et al.*, 1996) for the period after 2010 (P. James, 2016; personal communication).

In the automated classification, basic mean composites of atmospheric variables are made for each of the 29 pre-defined Grosswetterlagen, requiring that an ST lasts at least 2 days to remove less relevant transient weather patterns. This is modified from James (2007), who used a strict 3-day threshold. Daily pattern correlations between the mean composites and mean sea level pressure, precipitable water, 500–1000 hPa thickness, and 500 hPa geopotential height are applied to automatically assign days to the 29 STs. Each day is assigned to the ST with the highest correlation.

The SVG covers a larger domain than the Hess-Brezowsky Grosswetterlagen, but a smaller domain than the Objective-Grosswetterlagen (Hoy *et al.*, 2013a). It is not possible to define a boundary for the validity of the SVG because the pattern correlations are calculated with weights that gradually decay with distance from Central Europe. P. James (2014, personal communication) recommends using the domain 40°–65°N and 10°W–30°E. This is slightly smaller than the domain selected for this study. We show the results for all of Europe for completeness, while keeping in mind that the SVG classification is more robust for central parts of Europe. Hoy *et al.* (2013b) confirmed that the SVG adequately explains European temperature changes.

2.1.1. *Observed temperatures from WFDEI*

Temperature data for the study period (1981–2010) were taken from a bias-corrected reanalysis data set, the WFDEI (Weedon *et al.*, 2014). The WFDEI is a daily, gridded 0.5° data set of surface variables, originating from the ERA-Interim reanalysis (Dee *et al.*, 2011) and covering the period 1979–2012. It consists of instantaneous flux variables (air temperature, wind speed, surface pressure, and specific humidity) and accumulated flux variables (longwave and shortwave downward surface radiation fluxes, rainfall, and snowfall rate), available at 3-hourly and daily time steps. Here we use daily mean 2 m air temperatures.

Temperatures in the WFDEI were extracted from ERA-Interim every 3-h forecasts and interpolated to a regular 0.5° lat–lon grid before being elevation corrected using the environmental lapse rate and bias-corrected against gridded 0.5° monthly observations of average temperatures and diurnal temperature ranges from the Climate Research Unit (CRU), University of East Anglia. Prior to 2010, temperatures stem from CRU TS 3.1 (Harris *et al*., 2014, available from http://catalogue.ceda.ac.uk/). An updated version, CRU TS 3.21, was used for the period 2010–2012, affecting only the last year of our study

© 2016 Royal Meteorological Society

period. Weedon *et al.* (2014) report that using CRU TS 3.1 instead of CRU TS 3.21 results in minor differences across the global data set. The station coverage in CRU varies over time, but generally does not alter the average temperatures (Weedon *et al.*, 2014). Discontinuities and artificial variability make reanalysis data unsuitable for trend analyses (Simmons *et al.*, 2010; Saffioti *et al.*, 2015); however, CRU trends, not ERA-Interim trends, are preserved after bias-correction (G. Weedon, 2015; personal communication), making the WFDEI a good candidate for large-scale, gridded trend studies. In addition, it is worth noting that WFDEI variables are spatially consistent after bias-correction (Weedon *et al.*, 2014), which is important when linking the local climate to the large-scale synoptic situation. Validation of WFDEI (Weedon *et al.*, 2014) shows that daily temperatures agree well with observed surface fluxes at seven FLUXNET stations globally (of which three are European stations). Iizumi *et al.* (2014) conducted further validation, comparing WFDEI with the Global Summary of Day data set (Climate Prediction Center, 1987) and found little bias for average temperatures. WFDEI proved superior regarding daily mean temperature biases out of seven tested reanalysis and forcing data sets. The WFDEI was used for the European example, because it retains the accuracy of the underlying CRU data set, while improving spatial resolution and undergoing additional bias-correction using climate station observations.

3. Methods

3.1. Trend estimation

The first step in the study was to perform a trend analysis of WFDEI temperature changes across Europe. Temperature trends were calculated using the Sen slope (also called the Theil-Sen estimator or Kendall–Theil Robust Line; Theil, 1950; Déry *et al*., 2005), because this nonparametric trend estimator is less influenced by outliers than the linear regression line (Stahl *et al.*, 2012). The Mann–Kendall test (Sneyers, 1990) was used to assess whether the WFDEI trend is significantly different from zero (significance level 0.05). The magnitude of the WFDEI trend is hereafter referred to as m_{WFDEI}, which is derived as the median of the linear slopes between all pairs of values:

$$m = \text{median}\left[\frac{y_i - y_j}{t_i - t_j}\right] = \text{median}\left(m_k\right) \qquad (1)$$

where $yi - yj$ is the temperature difference between all possible values in the time series, $ti - tj$ is the corresponding time difference between each pair of values in the time series, and mk is a vector consisting of all possible linear slopes. All trends were calculated from $n = 30$ data points, both for annual averages and for each month separately (e.g. 30 mean January temperatures).

3.2. The probabilistic approach

The novel probabilistic approach provides a statistical test of whether the WFDEI temperature trend can be explained by changes in synoptic circulation alone. First, we derived the empirical distribution of synoptic-circulation-induced trends by repeated historical resampling. Second, we applied a test to assess the likelihood that the historical WFDEI trend could be randomly generated from this distribution, thereby assessing whether WFDEI trends can be explained by synoptic circulation changes alone.

3.2.1. Deriving synoptic-circulation-induced trends by resampling

Figure 1 (top) illustrates the main differences between the two procedures: (1) derivation of the hypothetical time series, following the existing Cahynová and Huth (2009) method of hypothetical trends, and (2) derivation of the resampled time series introduced in this study. Similar to the method of hypothetical trends, any day occurring in a given month with a given ST, will have the same temperature in the new constructed time series. Thus, STs are assumed not to warm or cool over time, which means that any changes in the hypothetical temperature series must be caused by changes in the frequency of STs over time. With this assumption, positive (negative) trends will result if warm (cool) STs become more frequent at the expense of cool (warm) STs. The resampled time series were derived as follows (for each grid cell sampled simultaneously):

(1) Randomly select 1 day from all days with a certain month *k* and ST *l*.
(2) Replace the temperature for all daily instances of ST *l* in month *k* with the temperature for this randomly selected day.
(3) Repeat the resampling and replacement for all combinations of months and STs.
(4) Calculate monthly mean temperatures for each grid cell using the resampled time series.
(5) Calculate monthly trends of timeseries of resampled temperature using the Sen slope (Section 3.1). The resulting trends are referred to as synoptic-circulation-induced trends.
(6) Repeat the resampling 10 000 times with replacement, implying that some days will be resampled in multiple realizations, whereas others may not be selected.

The resulting Sen slopes for each of the 10 000 ensemble time series comprise the resampled distribution of possible synoptic-circulation-induced trends for a given grid cell. The median of the distribution of synoptic-circulation-induced trends is referred to as m_{SC}. This distribution can then be used to test the likelihood that the WFDEI trend can be explained by changes in ST frequency alone.

3.2.2. Statistical test to attribute trends to changes in synoptic circulation alone

The likelihood that the WFDEI temperature trend belongs to the distribution of synoptic-circulation-induced trends is formulated as a two-sided, nonparametric Monte Carlo test (Besag and Diggle, 1977) with the following hypotheses:

© 2016 Royal Meteorological Society

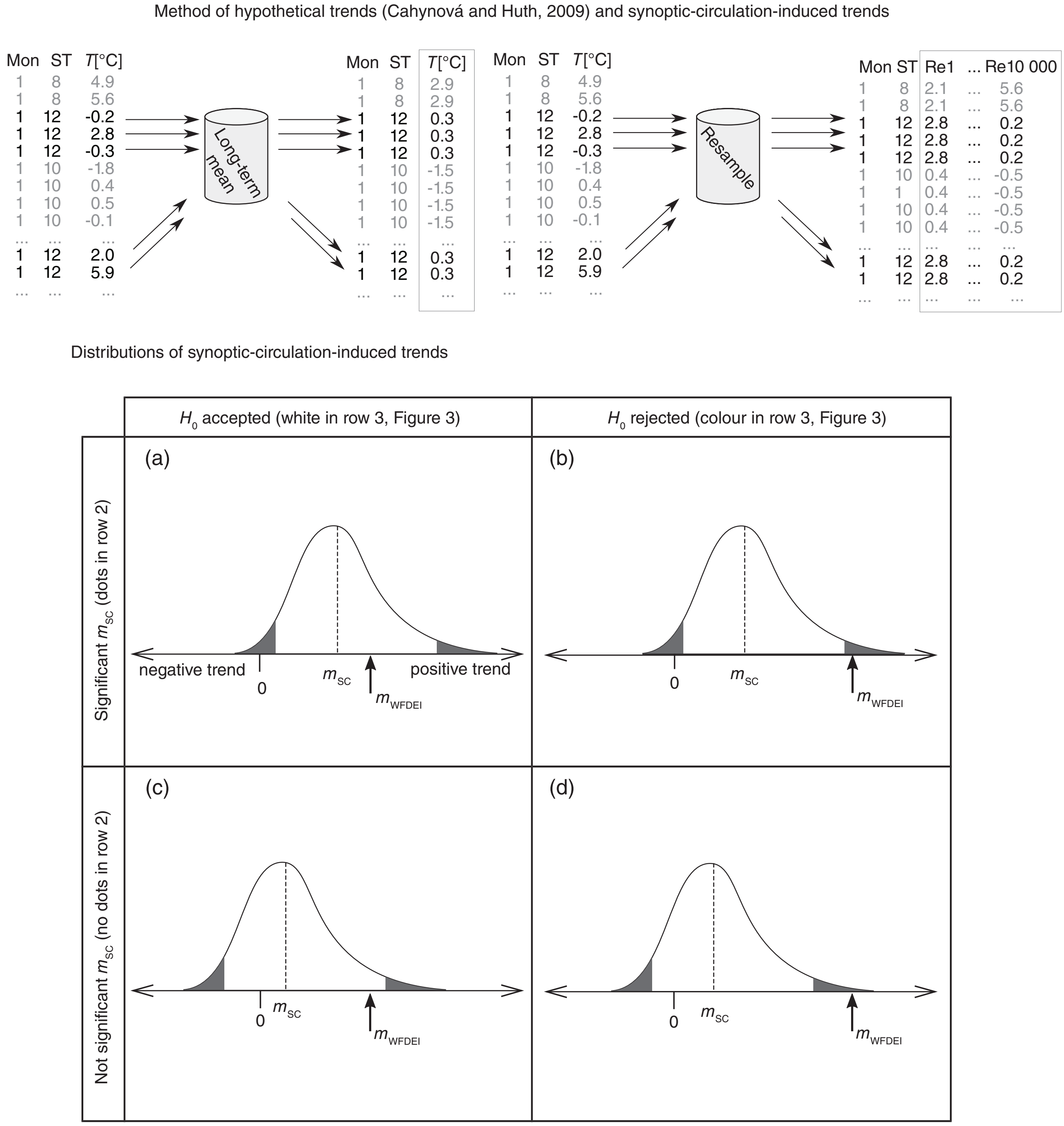

Figure 1. (top) Example of how to calculate synoptic-circulation-induced time series using the method of hypothetical trends (left) and our probabilistic approach (right). (bottom) The probabilistic approach allows comparing the WFDEI trend (m_{WFDEI}) to the distribution of synoptic-circulation-induced trends. If H_0 is accepted, the grid cell is white, the bottom rows in Figure 3 (panels (a) and (c)), and if H_0 is rejected, a colour is shown (panels (b) and (d)). If the distribution of synoptic-circulation-induced trends is significantly different from zero (significant m_{SC}), the grid cell is marked with a dot in the middle rows of Figure 3 (panels (a) and (b)), otherwise, no dot is shown (panels (c) and (d)).

H_0: The WFDEI trend can be explained by changes in synoptic circulation alone.

H_a: The WFDEI trend cannot be explained by changes in synoptic circulation alone.

The null hypothesis was tested by assessing the likelihood that the observed trend, m_{WFDEI}, could have occurred randomly from the distribution of synoptic-circulation-induced trends, resulting in a standard *p*-value. This is illustrated in Figure 1 (bottom). The left column shows two cases where the null hypothesis is accepted, implying that changes in synoptic circulation alone can explain the WFDEI trend. The two cases in the right column show cases where the null hypothesis is rejected, implying that m_{WFDEI}, is significantly different from the circulation-induced trends

© 2016 Royal Meteorological Society

and that other factors contribute to the WFDEI trend, in whole or in part. Rows in this figure test whether the synoptic-circulation-induced trends are significantly different from zero, with the top row showing a significant effect of synoptic-circulation-induced trends (hereafter: significant m_{SC}), and the bottom row demonstrating no significant effect of circulation trends (not significant m_{SC}). The four possible combinations listed in Figure 1 (bottom) allow a rigorous analysis of the results and provide a useful reference when visualizing gridded test results.

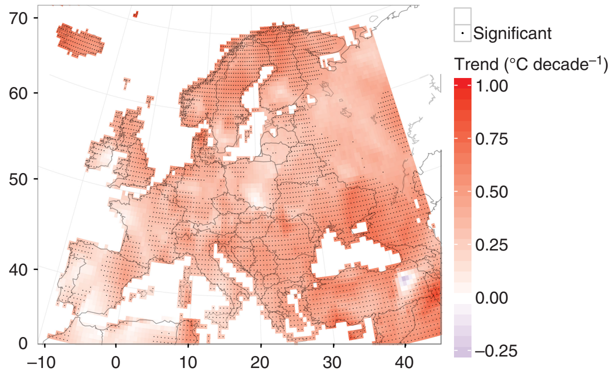

Figure 2. Trends (Sen slopes) of WFDEI temperature for the period 1981–2010 (annual average). The Sen slope was calculated as the median slope of all possible combinations of pairs in the annual mean of WFDEI temperatures. Dots mark significant temperature trends.

4. Results

This section presents an example analysis using the proposed trend attribution test for Europe. It provides a brief overview of the spatial pattern of the annual trends (Sen slopes) in WFDEI temperatures (1981–2010) in Section 4.1 and Figure 2, followed by a detailed analysis of the corresponding monthly trends and whether they can be attributed to changes in synoptic circulation alone. Monthly trends are shown in Figure 3(a) (for winter and spring) and Figure 3(b) (for summer and autumn), displaying the key result of the study in one figure. The different parts of this figure are explained in Sections 4.2–4.4. Colours in the top rows of Figure 3 show the trends in monthly historical WFDEI temperatures (m_{WFDEI}, as defined in Section 3.2.2.) and dots indicate where these historical trends are significant ($m_{WFDEI} \neq 0$). Colours in the middle rows show the synoptic-circulation-induced temperature trends (calculated as the median of the distribution, m_{SC}) and the presence of dots indicates where circulation-induced trends are significant ($m_{SC} \neq 0$, cases (a) and (b)). The third rows show the results of the significance test outlined in this article and informs whether synoptic circulation alone can explain the WFDEI trends. White regions show areas where the null hypothesis is accepted, i.e. m_{WFDEI} (cases (a) and (c)), whereas colours show regions where $m_{WFDEI} \neq m_{SC}$ (cases (b) and (d)). Trends towards higher temperature (warmer) are shown in red, whereas trends towards lower temperature (cooler) are shown in blue. Significant trends are marked as dots. For convenience, dots from the top row are reproduced in the bottom row so that the reader may focus on regions, which have significant WFDEI trends. Per this recommendation, the results presented in this section will focus on regions with significant WFDEI trends (dots in the bottom row) to determine whether the significant historical trend can be explained by circulation changes (white in the bottom row) or by additional within-type changes (colours in bottom row). By comparing the plots across all three rows and referring to the cases in Figure 1, it is possible to infer what is driving temperature changes in different regions and at different times of the year. We emphasize that the results are sensitive to the data and period chosen, nevertheless, the recent European temperature changes serve as a suitable testbed for the applicability of our novel probabilistic approach.

4.1. Trends in annual WFDEI temperature

Annual WFDEI trends were positive for nearly all of Europe except for a few isolated grid cells in Turkey (Figure 2). Warming trends were significant in 70.7% of the grid cells (Table 1), dominating southeastern and northwestern Europe. Averaged over all of Europe, the annual trend amounted to 0.4 °C decade^{-1}, ranging from −0.25 to 0.87 °C decade^{-1}.

4.2. Trends in monthly WFDEI temperature (top rows)

Monthly WFDEI trends are summarized in Figure 3 (top rows) and Table 1. Historical warming (m_{WFDEI}) was most widespread in summer, notably in August when >60% of the grid cells displayed significant warming. The summer months June and July showed a similar widespread warming (≈45%), followed by April and May (≈25–30%), and September and November (≈20%). The lowest fraction of grid cells experiencing significant warming was seen in the winter months (≈5%), when these significant trends were restricted to only northern regions. In May, the warming signal dominated southwestern Europe, and in June, it was seen across Central Europe. In July and August, significant warming was found further east, extending from the northern to the southern borders of the domain. In September and October, only small areas, Scandinavia and southeastern Europe respectively, were affected, whereas in November, large parts of southeastern Europe were again shown to be significantly warming. Localized warming patterns existed in Scandinavia (January and December), in the British Isles (January), and in Iceland (January, June–September, and December). Significant cooling was found in a few grid cells for Turkey in January (likely caused by spurious data errors, see Section 5.5), and for Spain in November and December. In the latter case, these grid cells were part of a larger pattern of cooling, covering Western Europe. Similar large-scale cooling patterns were also found in other months and regions; however, none of these showed any significance and are therefore not discussed further. Note also that the threshold for what is considered significant will vary with grid cell and month.

© 2016 Royal Meteorological Society

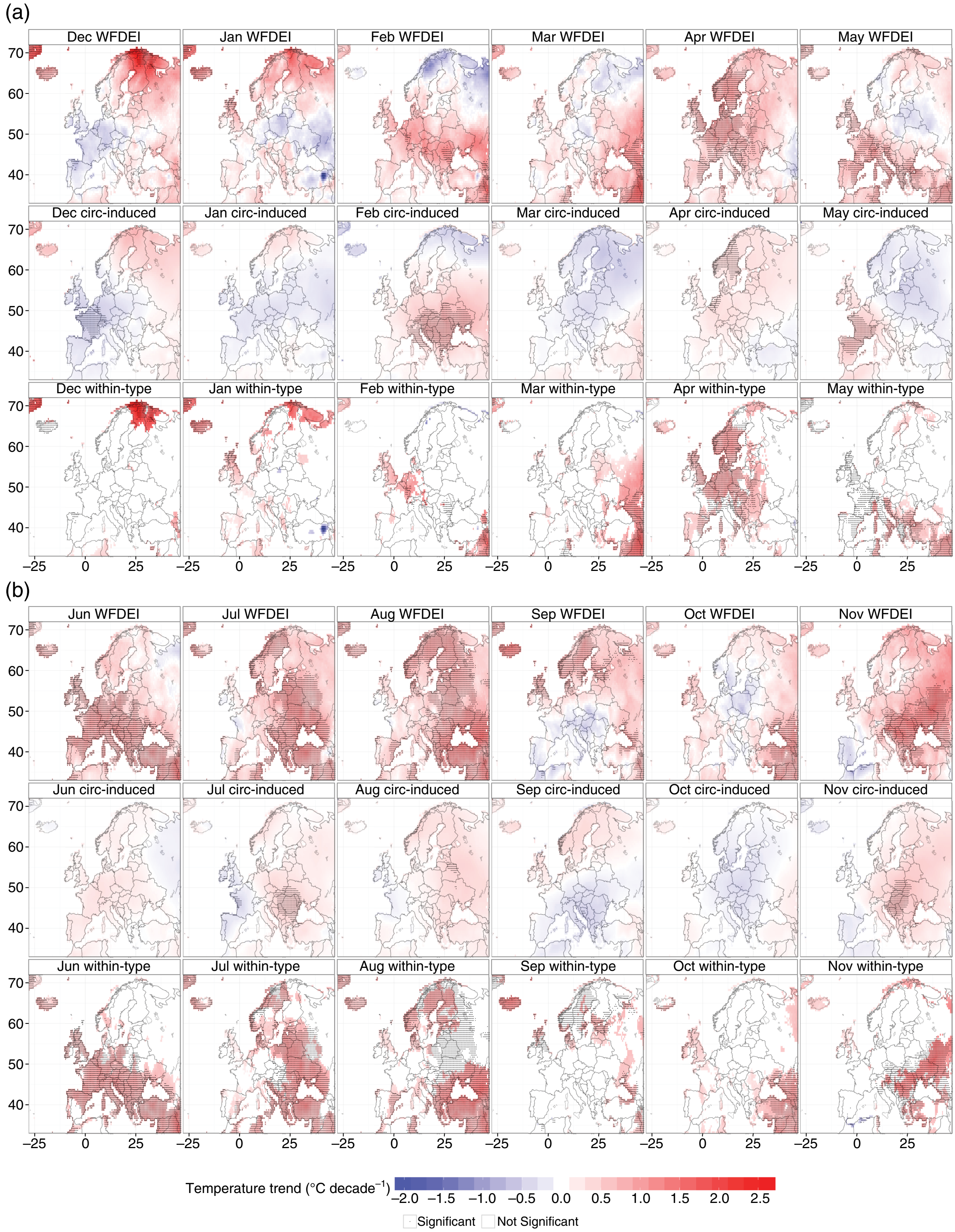

Figure 3. WFDEI trends for (a) winter and spring, and (b) summer and autumn. Top row: WFDEI temperature trends for the period 1981–2010. Dots mark significant WFDEI trends. Middle row: median of the (resampled) synoptic-circulation-induced trends (m_{SC}). Dots mark significant synoptic-circulation-induced temperature trends. Bottom row: as the top row, but with white regions to indicate where the Monte Carlo test is accepted (i.e. explained by synoptic circulation changes alone), coloured regions where the null hypothesis is rejected (i.e. other factors play a role).

© 2016 Royal Meteorological Society

Table 1. Number and fraction of grid cells (out of 6352 grid cells in total) that experience significant warming (left), cooling (middle), and that which cannot be explained by circulation changes alone (right), i.e. the null hypothesis is rejected.

	Mann–Kendall trend test		Monte Carlo test
	Significant warming (%)	Significant cooling (%)	Rejected H_0 (%)
January	4.8	0.2	27.1
February	5.1	0	13.8
March	10.3	0	30.0
April	29.4	0	43.9
May	25.4	0	22.0
June	43.7	0	50.2
July	46.2	0	53.4
August	60.3	0	47.4
September	22.0	0.3	20.4
October	13.6	0	31.6
November	23.5	0.4	26.4
December	6.2	0.4	10.5
Annual	70.7	–	–

For example, the critical thresholds in winter and summer (top rows) are not necessarily equal across months, because winter has a higher temporal variability than summer.

4.3. Derived synoptic-circulation-induced trends (middle rows)

Synoptic-circulation-induced trends, i.e. the component of the WFDEI trend that can be attributed to changes in the frequency of STs, are plotted in the middle rows of Figure 3. The median of the distribution of synoptic-circulation-induced trends (m_{SC}) is shown in colour in the middle rows. Additional dots indicate that the distribution of synoptic-circulation-induced trends were significantly different from zero (significant m_{SC}). By comparing regions of significant WFDEI trends (dotted regions in the top rows) with regions in the middle row, we see that significant warming WFDEI trends could be explained by more frequent warm STs for Scandinavia and Benelux in April; France and Spain in May; the Balkans, Ukraine, and Hungary in July; and southeastern Europe in November. More localized significant WFDEI trends were combined with significant m_{SC} in the Balkans and north Italy in February, Belarus in August, and Western Norway in September. In December, we could see a cooling WFDEI trend in Spain and significant m_{SC} in France. Even though the m_{SC} was not significant in Spain, the proximity to the larger signal of synoptic-circulation-induced cooling in France suggests that the cooling in Spain in December may be influenced by synoptic circulation changes.

Warming and cooling patterns of synoptic-circulation-induced trends generally resembled those of the WFDEI trends (comparing the upper and middle rows), however, the magnitudes of m_{SC} were generally weaker than m_{WFDEI}. This is because m_{WFDEI} represents one realization, whereas m_{SC} represents the ensemble median of 10 000 realizations. Thus, m_{SC} is smoothed compared to m_{WFDEI} because the variance of the sample median is reduced as the number of samples increases. It should further be noted that in some specific cases, the two trend magnitudes disagree in sign. In certain months and regions, such as the Baltics in March, Scandinavia in May, and Spain in July, synoptic-circulation-induced trends were negative, whereas WFDEI trends were positive. Here, the cooling imposed by synoptic circulation changes is exceeded by other factors, resulting in an observed warming trend.

4.4. Attributing trends to synoptic circulation changes or within-type changes (bottom rows)

The result of the Monte Carlo test is shown in the bottom rows of Figure 3. They show the same as the top rows, except that white regions indicate where the Monte Carlo test is accepted. Thus, significance dots on top of white indicate that a significant temperature trend can be explained by synoptic circulation changes alone, and significance dots on colour indicate that other factors play a role in creating a significant temperature trend. Here we discuss how the results jointly explain the relative role of synoptic circulation changes, focusing on regions with significant WFDEI trends (dots in the bottom row), and sort the results into the four cases shown in Figure 1.

Significant WFDEI warming detected in April, June, July, and August across Europe could not be explained by synoptic circulation trends and therefore within-type changes played an important role in the large-scale warming during these spring and summer months. These within-type trends correspond to case (d) in Figure 1, and emerge because the null hypothesis is rejected, and m_{SC} is not significant. Table 1 (right columns) shows that the null hypothesis is rejected in >40% of the grid cells in these months. In the southeastern part of the domain, within-type changes also played a role in March, May, October, and November. To a smaller extent, within-type changes explained the warming in December and January for Northern Scandinavia, May for Eastern Mediterranean, and in March and October east of the Black Sea. In March, June, and October, there was nearly a 1 : 1 correspondence between the WFDEI trend and the within-type trend signal.

The WFDEI trend was explained by synoptic circulation changes alone (case (a) in Figure 1) in France and Spain in May. In the Balkans in February and Belarus in August, this case covered small regions of significant WFDEI trends. These trends can be explained by more frequent warm and less frequent cool STs over the time period. Both synoptic circulation changes and within-type changes contributed to the trend for Scandinavia and Benelux in April (case (b)). Case (c) was found for the Baltics in August and for Scandinavia in September. Here, synoptic circulation changes explain the WFDEI trend, but the distribution of synoptic-circulation-induced trends is not significant at the 0.05 level.

© 2016 Royal Meteorological Society

5. Discussion

5.1. Trends in WFDEI temperature

Trends in annual and monthly WFDEI temperature showed clear warming across most of Europe in agreement with previously published trend patterns (EEA, 2008; Simmons *et al.*, 2010; Jones *et al.*, 2012). Annually, we found a strong warming signal in Northern and Eastern Europe, as also found by EEA (2008), Simmons *et al.* (2010), and Jones *et al.* (2012) for the periods 1976–2006, 1979–2008, and 1951–2010, respectively. Seasonally, the most widespread warming across Europe was found from June to August, in April, and in November, as also reported by Fleig *et al.* (2015) for the period 1957–2001. Significant cooling was only detected in a few individual grid cells.

The strongest trend magnitudes were seen in a rather small region in the northernmost part of Scandinavia, with trends of up to 2.6 °C decade^{-1} in December. This strong warming may be influenced by limited station coverage, and poor data quality during winter. To investigate this further, we compared temperature trends in WFDEI against trends in station observations. The results (not shown) confirmed strong trends on the order of 2 °C decade^{-1} during December and January. Certain stations in Norway used by CRU are known to be influenced by temperature inversions (Vikhamar-Schuler and Hanssen-Bauer, 2010). Therefore, temperature trends at these stations likely reflect that temperature inversions have become less frequent rather than a general warming of the region. Thus, whether these results are representative for a larger region remains an open question.

We found relatively small regions of significant warming WFDEI trends in winter, contrary to previous studies (Klein Tank *et al.*, 2005; Fleig *et al.*, 2015). There are several reasons for this, including differences in time periods and data used. Winter warming from the 1960s to the 1990s is commonly explained by a positive phase in the North Atlantic Oscillation (NAO), favouring more frequent westerly (warm) STs and less frequent easterly (cool) STs (Brönnimann *et al.*, 2009; Cahynová and Huth, 2009; Cattiaux *et al.*, 2013; Hoy *et al.*, 2013a). The time periods used by Fleig *et al.* (2015) and Klein Tank *et al.* (2005) (1963–2001 and 1976–1999, respectively) ended when NAO was in its positive phase, whereas our study period (1981–2010) extends into the recent downward trend in NAO during the last decade, including the very cold winter 2009/2010 (Hurrell and Deser, 2009; Osborn, 2011). Saffioti *et al.* (2015) reported that from 1998 to 2012, temperature trends during winter in the mid-latitudes of Europe became negative, partly because of this shift in the synoptic circulation, i.e. towards cooling in Northern Europe. They further argued that the Northern Hemisphere winter cooling was overestimated because of incomplete observation coverage in the warming Arctic. This warming hiatus partly explains why pronounced winter warming was rather limited in our study.

5.2. Trends attributed to synoptic circulation changes alone (H_0 accepted)

In this section, we discuss to what degree WFDEI trends can be attributed to synoptic circulation changes alone. The null hypothesis, H_0, was accepted and m_{SC} was significant in May for France and Spain (case (a) in Figure 1). Fleig *et al.* (2015) reported similar strong influences of synoptic circulation on temperature in May for France and the UK, however, they found the highest trend ratios (implying dominating influence of synoptic circulation changes) in January and February for Western Europe, and in November for the Balkans. Further, Fleig *et al.* (2015) found no circulation influence for the Baltics in August or for Scandinavia in September (where we found that H_0 was accepted, but m_{SC} was not significant at the 0.05 level).

Previous studies report the NAO to be the most important mode of atmospheric variability for Europe (e.g. Hurrell and Deser, 2009; Hertig *et al.*, 2015). NAO impacts temperatures most strongly in winter, and its impact is greatest for North Atlantic Europe (Beranová and Huth, 2008; Hurrell and Deser, 2009). During its positive phase, NAO advects warm air to Northern Europe and cold air to Southern Europe, however, the correlation between NAO and temperature is non-stationary in time (Hertig *et al.*, 2015). Beranová and Huth (2008) analysed relationships between five modes of variability and maximum winter temperatures for all of Europe over the period 1958–1998 and found that increased zonality caused an eastward shift of the Icelandic low during the positive phase of NAO. This shift led to more cyclonic situations north of 45°N, and an eastward shift of the Azores high that led to more anticyclonic situations south of 45°N. A number of circulation classifications have been applied to study circulation changes across Europe in recent decades, including the Grosswetterlagen (1958–2000; Kyselý and Huth, 2006); the SANDRA scheme (1850–2003; Philipp *et al.*, 2007); the Objective-Grosswetterlagen (1960–2002; James, 2007); the SVG, Grosswetterlagen and Vangenheim-Girs (1901–2010 and 1981–2010; Hoy *et al.*, 2013a); and COST733cat classifications (1961–2000; Cahynová and Huth, 2016). For a summary of circulation classifications tested in the COST733 Action, see Huth *et al.* (2008). The study periods differ, but the results are nevertheless consistent in winter and, to some degree, in other seasons. In winter, mild westerly STs have increased, whereas cold easterly types have decreased (Kyselý and Huth, 2006; Philipp *et al.*, 2007; Hoy *et al.*, 2013a; Cahynová and Huth, 2016), confirming winter warming (Jones and Lister, 2009; Hoy *et al.*, 2013b). Anticyclonic types and the frequency of blockings increased until 1990 and declined thereafter, favouring more extreme temperatures in the first period (Kyselý and Huth, 2006). In spring, no clear changes in the ST frequencies were found (Philipp *et al.*, 2007; Cahynová and Huth, 2016). In April and the summer months, Hoy *et al.* (2013a) found that synoptic circulation explained a part of the warming signal by an increase in continental, anticyclonic situations that attracted warm air towards Central Europe, when comparing the periods 1981–2010 and 1901–2010. This coincides with the

© 2016 Royal Meteorological Society

widespread warming we found in Central Europe, however, except for July, we did not detect clear influence of synoptic-circulation-induced changes on this widespread warming. In summer, cool northerlies increased (Philipp *et al.*, 2007), however, Kyselý and Huth (2006) found that they decreased after mid 1980s. In autumn, cool STs decreased (Philipp *et al.*, 2007). Cahynová and Huth (2016) found no trend in ST frequency in spring, summer, or autumn, but still detected temperature changes in those seasons.

We made an effort to detect changes of individual ST frequencies that could help elaborate on change patterns related to synoptic circulation (middle rows of Figure 3). This was not possible, however, because of methodological issues. It was concluded that a rigorous analysis of changes in the ST frequencies would require a regional-based approach for all months, which is beyond the scope of this study.

5.3. Trends attributed to within-type changes (H_0 rejected)

Here we discuss the two cases arising when WFDEI trends that could not be explained by synoptic circulation changes alone: H_0 rejected and significant m_{SC} (case (b)) and H_0 rejected, but synoptic circulation changes were not significant on the 0.05 level (m_{SC} not significant; case (d)). Case (b) was detected for Scandinavia in April, and for the Balkans in July and November. The combined influence of the two components have been documented by Jones and Lister (2009), who found that certain STs experiencing within-type change also increased in frequency (Philipp *et al.*, 2007). For the Balkans in November, cool STs became more frequent (Fleig *et al.*, 2015). For Scandinavia, they found an increasing trend of dry, warm STs in April; however, the signal was not significant. Contrary to our findings of synoptic-circulation-induced trends, Fleig *et al.* (2015) reported negligible synoptic circulation influences for Scandinavia in April, and the Black Sea region in July, likely because of the different time periods used.

Case (d) was detected for large parts of Europe from April to August, and north of the Black Sea in November. These results are in line with other studies that found within-type changes to be important for Central Europe, especially in July (1780–1995; Beck *et al.*, 2007 and 1750–2000; Küttel *et al.*, 2011). It is worth noting that these studies are not directly comparable to ours because of the different time periods and methods. Both used objective circulation classifications based on mean sea level pressure. Further, they found marked multidecadal variability in the contribution of synoptic circulation changes and within-type changes over time, emphasizing that the results presented in section 4 are valid only for the time period analysed (1981–2010).

Within-type changes may be caused by positive feedbacks between the land surface and the atmosphere, by forcing from greenhouse gases, or other potential climate factors. Warming in water-limited regions during the summer has been documented to be influenced by soil moisture–temperature feedbacks (Vautard and Yiou, 2009; Zampieri *et al.*, 2009; Seneviratne *et al.*, 2010; Fischer *et al.*, 2012), which may explain the within-type changes we detected in Southern and Central Europe in spring and summer. The warming in Scandinavia during spring and summer is likely influenced by albedo feedbacks related to changes in snow cover and/or vegetation cover, and potentially also soil moisture feedbacks. Reduced snow cover and a longer growing season have been documented for Norway by Wilson *et al.* (2010), Skaugen *et al.* (2012), and Dyrrdal *et al.* (2013). Near the Atlantic coast, sea surface temperatures have been found to influence air temperatures, through direct heating of air masses (de Bilt, The Netherlands, for 2006; van Oldenborgh, 2007 and Central England temperatures, 1850–2007; Parker, 2009). We performed a trend analysis of the Extended reconstructed sea surface temperature (ERSST) data set (Sen slopes for the period 1981–2010, for all of Europe; not shown). It did not reveal pronounced trends in the Barents Sea in any of the months, but warming trends were detected in the Bay of Bothnia from January to September.

5.4. Confirmation of within-type changes

To further investigate the role of within-type changes, we selected the Black Sea region in November as a region experiencing significant WFDEI trends where the null hypothesis was rejected. Figure 4 shows trends (Sen slopes) in three temperature groups of STs: the warmest, medium, and coldest one-third of the ST mean temperature. With as many as 29 STs, it was necessary to group STs to get enough samples for a trend analysis. Temperature trends of these ST groups were subsequently calculated. A single ST may result in low temperatures for some regions and high for others, therefore, the grouping was done for a region that was assumed to be rather homogeneous in terms of synoptic circulation influence (grey box in Figure 4). All three ST groups in November warmed over time, confirming that within-type changes play a role. Temperatures in the warm ST group increased more than in the medium and cold groups.

This test for the Black Sea region in November, as well as the within-type changes detected in spring and summer, shows that a predictable link between synoptic circulation and the local climate is not always present. Predictions of local temperature from synoptic circulation, for instance in statistical downscaling, require such a predictable link (Beck *et al.*, 2007). For months and regions experiencing within-type changes, care should be taken before applying statistical downscaling.

5.5. Uncertainty

As a primarily methodological study, the analysis presented here focused on large-scale consistent patterns, while largely discounting isolated anomalies as a topic for later study. While the WFDEI temperature data are among the best available high resolution data sets available for Europe, some of the localized trends may be

© 2016 Royal Meteorological Society

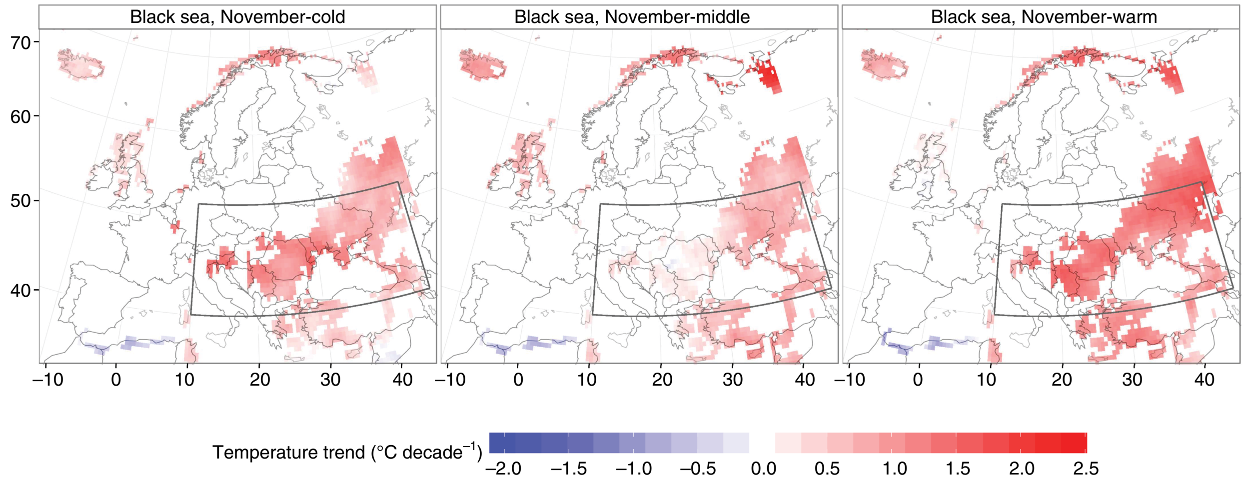

Figure 4. Sen slopes for the warmest, middle, and coldest one-third of the STs, for the Black Sea region in November. Grid cells influenced by changes in synoptic circulation are not shown, to limit the analysis to within-type change. The definition of a cold and warm ST is not valid outside the grey box.

related to underlying issues in the data set. Some CRU stations used in the bias-correction contain time series unsuitable for trend analyses. This is likely caused by quality issues, such as long periods of missing data. For example, the Turkish mountain station Erzurum lacks data for 10 months during the period 1987–1991 and Almeria in Spain lacks data for 8 months in 1980 (Jones *et al.*, 2012). In CRU, missing observations are replaced by the climatological mean monthly temperature, which may introduce biases in grid cells that often lack observations (Weedon *et al.*, 2014). This may explain some highly localized trends, particularly near the Eastern Turkey site that operate differently than the predominant regional trends and remain a topic for more detailed, regional confirmation. Concerning the validity of the SVG data set, it must be kept in mind that its performance decays with distance from Central Europe (i.e. Germany), implying higher uncertainty towards the outer boundary of the domain.

6. Conclusions

The aim of this study is to introduce a novel probabilistic approach to detect months and regions where recent temperature trends can be explained by changes in atmospheric synoptic circulation alone. The approach has been developed based on data for Europe (1981–2010), but is applicable in any region of the world, as well as for other variables. Temperatures, available from the WFDEI, and a catalogue of STs (SVG) were used to assess changes in the frequency of STs. The probabilistic approach, which involves resampling and a Monte Carlo test, allows assessing the spread of synoptic-circulation-induced trends and thereby provides an estimate of the likelihood that the WFDEI temperature trend is attributable to changes in synoptic circulation alone. The approach represents a notable improvement to limitations inherent in existing methodologies.

The main conclusions are:

- Widespread warming in annual temperature was found in large parts (70%) of Europe, and in all months. The most consistent warming signal was found from April to August, and in November, affecting large parts of continental Europe. In winter, the extent was smallest, but the trend magnitudes were strongest.
- Synoptic-circulation-induced trends, i.e. the part of the trend that can be attributed to changes in the frequency of STs, were important for explaining warming trends for Western Europe in May. For the Baltics in August, and Scandinavia in September, synoptic circulation changes explained the warming, but the distribution of synoptic-circulation-induced trends was not significantly different from zero.
- Within-type changes, i.e. STs changing their properties over time, explained the warming trends in April, June, July, and August for much of continental Europe, and north of the Black Sea in November.
- Both circulation changes and within-type changes influenced WFDEI trends in April (Scandinavia), July, and November (the Balkans).
- For the Black Sea region in November, we showed that STs warmed over time, confirming the role of within-type changes.

To investigate the physical processes controlling the detected changes requires targeted land surface model experiments, preferably in combination with flux measurements. This is the topic for further studies.

Acknowledgements

The authors wish to thank P. James (Deutscher Wetterdienst, Offenbach, Germany) for providing the SVG STs and the FRIEND-Water community for exchange of ideas and experience. We thank the reviewers for their valuable comments.

© 2016 Royal Meteorological Society

References

Barry RG, Perry AH. 1969. 'Weather-type' frequencies and the recent temperature fluctuation. *Nature* **222**(5192): 463–464, doi: 10.1038/222463a0.

Baur F, Hess P, Nagel H. 1944. Kalender der Grosswetterlagen Europas 1881–1939. Technical Report, Forschungsinstitut für langfristige Witterungsvorhersage, Bad Homburg, Germany.

Beck C, Jacobeit J, Jones PD. 2007. Frequency and within-type variations of large-scale circulation types and their effects on low-frequency climate variability in central Europe since 1780. *Int. J. Climatol.* **27**(4): 473–491, doi: 10.1002/joc.1410.

Beranová R, Huth R. 2008. Time variations of the effects of circulation variability modes on European temperature and precipitation in winter. *Int. J. Climatol.* **28**(2): 139–158, doi: 10.1002/joc.1516.

Besag J, Diggle PJ. 1977. Simple Monte Carlo tests for spatial pattern. *J. R. Stat. Soc. Ser. C Appl. Stat.* **26**(3): 327–333, doi: 10.2307/2346974.

Bindoff N, Stott P, AchutaRao K, Allen M, Gillett N, Gutzler D, Hansingo K, Hegerl G, Hu Y, Jain S, Mokhov I, Overland J, Perlwitz J, Sebbari R, Zhang X. 2013. *Detection and Attribution of Climate Change: From Global to Regional*, book section 10. Cambridge University Press, ISBN 978-1-107-66182-0: Cambridge, UK and New York, NY, 867–952, doi: 10.1017/CBO9781107415324.022.

Brönnimann S, Stickler A, Griesser T, Fischer AM, Grant A, Ewen T, Zhou T, Schraner M, Rozanov E, Peter T. 2009. Variability of large-scale atmospheric circulation indices for the Northern Hemisphere during the past 100 years. *Meteorol. Z.* **18**(4): 379–396, doi: 10.1127/0941-2948/2009/0389.

Cahynová M, Huth R. 2009. Changes of atmospheric circulation in central Europe and their influence on climatic trends in the Czech Republic. *Theor. Appl. Climatol.* **96**(1): 57–68, doi: 10.1007/s00704-008-0097-2.

Cahynová M, Huth R. 2010. Circulation vs. climatic changes over the Czech Republic: a comprehensive study based on the COST733 database of atmospheric circulation classifications. *Phys. Chem. Earth Pt. A/B/C* **35**(9–12): 422–428, doi: 10.1016/j.pce.2009.11.002.

Cahynová M, Huth R. 2016. Atmospheric circulation influence on climatic trends in Europe: an analysis of circulation type classifications from the COST733 catalogue. *Int. J. Climatol.* **36**(7): 2743–2760, doi: 10.1002/joc.4003.

Cattiaux J, Douville H, Ribes A, Chauvin F, Plante C. 2013. Towards a better understanding of changes in wintertime cold extremes over Europe: a pilot study with CNRM and IPSL atmospheric models. *Clim. Dyn.* **40**(9–10): 2433–2445, doi: 10.1007/s00382-012-1436-7.

Christensen J, Krishna Kumar K, Aldrian E, An SI, Cavalcanti I, de Castro M, Dong W, Goswami P, Hall A, Kanyanga J, Kitoh A, Kossin J, Lau NC, Renwick J, Stephenson D, Xie SP, Zhou T. 2013. *Climate Phenomena and Their Relevance for Future Regional Climate Change*, book section 14. Cambridge University Press, ISBN 978-1-107-66182-0: Cambridge, UK and New York, NY, 1217–1308, doi: 10.1017/CBO9781107415324.028.

Climate Prediction Center. 1987. *CPC global summary of day/month observations, 1979-continuing*. http://rda.ucar.edu/datasets/ds512.0/ (accessed 20 May 2016).

Cohen J, Screen JA, Furtado JC, Barlow M, Whittleston D, Coumou D, Francis J, Dethloff K, Entekhabi D, Overland J, Jones J. 2014. Recent Arctic amplification and extreme mid-latitude weather. *Nat. Geosci.* **7**(9): 627–637, doi: 10.1038/ngeo2234. Review.

Compo GP, Whitaker JS, Sardeshmukh PD, Matsui N, Allan RJ, Yin X, Gleason BE, Vose RS, Rutledge G, Bessemoulin P, Brönnimann S, Brunet M, Crouthamel RI, Grant AN, Groisman PY, Jones PD, Kruk MC, Kruger AC, Marshall GJ, Maugeri M, Mok HY, Nordli O, Ross TF, Trigo RM, Wang XL, Woodruff SD, Worley SJ. 2011. The twentieth century reanalysis project. *Q. J. R. Meteorol. Soc.* **137**(654): 1–28, doi: 10.1002/qj.776.

Corti S, Molteni F, Palmer TN. 1999. Signature of recent climate change in frequencies of natural atmospheric circulation regimes. *Nature* **398**(6730): 799–802, doi: 10.1038/19745.

Dee DP, Uppala SM, Simmons AJ, Berrisford P, Poli P, Kobayashi S, Andrae U, Balmaseda MA, Balsamo G, Bauer P, Bechtold P, Beljaars ACM, van de Berg L, Bidlot J, Bormann N, Delsol C, Dragani R, Fuentes M, Geer AJ, Haimberger L, Healy SB, Hersbach H, Hólm EV, Isaksen L, Kållberg P, Köhler M, Matricardi M, McNally AP, Monge-Sanz BM, Morcrette JJ, Park BK, Peubey C, de Rosnay P, Tavolato C, Thépaut JN, Vitart F. 2011. The ERA-Interim reanalysis: configuration and performance of the data assimilation system. *Q. J. R. Meteorol. Soc.* **137**(656): 553–597, doi: 10.1002/qj.828.

Déry SJ, Stieglitz M, McKenna EC, Wood EF. 2005. Characteristics and trends of river discharge into Hudson, James, and Ungava Bays, 1964–2000. *J. Clim.* **18**: 2540–2557, doi: 10.1175/jcli3440.1.

Dyrrdal AV, Saloranta T, Skaugen T, Stranden HB. 2013. Changes in snow depth in Norway during the period 1961–2010. *Hydrol. Res.* **44**(1): 169–179, doi: 10.2166/nh.2012.064.

EEA. 2008. Impacts of Europe's changing climate – 2008 indicator-based assessment. EEA Report No. 4/2008, Copenhagen. www.eea.europa.eu/publications/eea_report_2008_4 (accessed 15 December 2015).

EEA. 2015. *Global and European Temperatures*. European Environment Agency: Copenhagen. www.eea.europa.eu/data-and-maps/indicators/global-and-european-temperature-1/assessment (accessed 15 December 2015).

Fischer EM, Rajczak J, Schär C. 2012. Changes in European summer temperature variability revisited. *Geophys. Res. Lett.* **39**(19): L19-702, doi: 10.1029/2012GL052730.

Fleig AK, Tallaksen LM, James P, Hisdal H, Stahl K. 2015. Attribution of European precipitation and temperature trends to changes in synoptic circulation. *Hydrol. Earth Syst. Sci.* **19**(7): 3093–3107, doi: 10.5194/hess-19-3093-2015.

Harris I, Jones PD, Osborn TJ, Lister DH. 2014. Updated high-resolution grids of monthly climatic observations – the CRU TS3.10 Dataset. *Int. J. Climatol.* **34**(3): 623–642, doi: 10.1002/joc.3711.

Hartmann D, Klein Tank A, Rusticucci M, Alexander L, Brönnimann S, Charabi Y, Dentener F, Dlugokencky E, Easterling D, Kaplan A, Soden B, Thorne P, Wild M, Zhai P. 2013. *Observations: Atmosphere and Surface*, book section 2. Cambridge University Press, ISBN 978-1-107-66182-0: Cambridge, UK and New York, NY, 159–254, doi: 10.1017/CBO9781107415324.008.

Hertig E, Beck C, Wanner H, Jacobeit J. 2015. A review of non-stationarities in climate variability of the last century with focus on the North Atlantic–European sector. *Earth Sci. Rev.* **147**: 1–17, doi: 10.1016/j.earscirev.2015.04.009.

Hess P, Brezowsky H. 1977. Katalog der Großwetterlagen Europas 1881–1976, 3rd edn. Technical Report Berichte des Deutschen Wetterdienstes 113, Deutscher Wetterdienst, Offenbach am Main, Germany.

Hoy A, Sepp M, Matschullat J. 2013a. Atmospheric circulation variability in Europe and northern Asia (1901 to 2010). *Theor. Appl. Climatol.* **113**(1–2): 105–126, doi: 10.1007/s00704-012-0770-3.

Hoy A, Sepp M, Matschullat J. 2013b. Large-scale atmospheric circulation forms and their impact on air temperature in Europe and northern Asia. *Theor. Appl. Climatol.* **113**(3–4): 643–658, doi: 10.1007/s00704-012-0813-9.

Hurrell JW, Deser C. 2009. North Atlantic climate variability: the role of the North Atlantic Oscillation. *J. Mar. Syst.* **78**(1): 28–41, doi: 10.1016/j.jmarsys.2008.11.026.

Huth R, Beck C, Philipp A, Demuzere M, Ustrnul Z, Cahynová M, Kyselý J, Tveito OE. 2008. Classifications of atmospheric circulation patterns. *Ann. N. Y. Acad. Sci.* **1146**(1): 105–152, doi: 10.1196/annals.1446.019.

Iizumi T, Okada M, Yokozawza M. 2014. A meteorological forcing data set for global crop modeling: development, evaluation, and intercomparison. *J. Geophys. Res. Atmos.* **119**(2): 363–384, doi: 10.1002/2013JD020130.

James PM. 2007. An objective classification method for Hess and Brezowsky Grosswetterlagen over Europe. *Theor. Appl. Climatol.* **88**(1): 17–42, doi: 10.1007/s00704-006-0239-3.

Jones PD, Lister DH. 2009. The influence of the circulation on surface temperature and precipitation patterns over Europe. *Clim. Past* **5**(2): 259–267, doi: 10.5194/cp-5-259-2009.

Jones PD, Lister DH, Osborn TJ, Harpham C, Salmon M, Morice CP. 2012. Hemispheric and large-scale land-surface air temperature variations: an extensive revision and an update to 2010. *J. Geophys. Res. Atmos.* **117**(D5): D05-127, doi: 10.1029/2011JD017139.

Kalnay E, Kanamitsu M, Kistler R, Collins W, Deaven D, Gandin L, Iredell M, Saha S, White G, Woollen J, Zhu Y, Leetmaa A, Reynolds R, Chelliah M, Ebisuzaki W, Higgins W, Janowiak J, Mo KC, Ropelewski C, Wang J, Jenne R, Joseph D. 1996. The NCEP/NCAR 40-year reanalysis project. *Bull. Am. Meteorol. Soc.* **77**(3): 437–471, doi: 10.1175/1520-0477(1996)077<0437:TNYRP>2.0.CO;2.

Klein Tank AMG, Können GP, Selten FM. 2005. Signals of anthropogenic influence on European warming as seen in the trend patterns of daily temperature variance. *Int. J. Climatol.* **25**(1): 1–16, doi: 10.1002/joc.1087.

Küttel M, Luterbacher J, Wanner H. 2011. Multidecadal changes in winter circulation-climate relationship in Europe: frequency variations, within-type modifications, and long-term trends. *Clim. Dyn.* **36**(5–6): 957–972, doi: 10.1007/s00382-009-0737-y.

Kyselý J, Huth R. 2006. Changes in atmospheric circulation over Europe detected by objective and subjective methods. *Theor. Appl. Climatol.* **85**(1–2): 19–36, doi: 10.1007/s00704-005-0164-x.

Leathers DJ, Ellis AW. 1996. Synoptic mechanisms associated with snowfall increases to the lee of lakes Erie and Ontario. *Int. J. Climatol.* **16**(10): 1117–1135, doi: 10.1002/(SICI)1097-0088(199610)16:10<1117::AID-JOC80>3.0.CO;2-4.

van Oldenborgh GJ. 2007. How unusual was autumn 2006 in Europe? *Clim. Past* **3**(4): 659–668, doi: 10.5194/cp-3-659-2007.

Osborn TJ. 2011. Winter 2009/2010 temperatures and a record-breaking North Atlantic Oscillation index. *Weather* **66**(1): 19–21, doi: 10.1002/wea.660.

Parker DE. 2009. Anomalies of Central England temperature classified by air source. *J. Clim.* **22**(5): 1069–1081, doi: 10.1175/2008JCLI2250.1.

Philipp A, Della-Marta PM, Jacobeit J, Fereday DR, Jones PD, Moberg A, Wanner H. 2007. Long-term variability of daily North Atlantic–European pressure patterns since 1850 classified by simulated annealing clustering. *J. Clim.* **20**(16): 4065–4095, doi: 10.1175/JCLI4175.1.

Saffioti C, Fischer EM, Knutti R. 2015. Contributions of atmospheric circulation variability and data coverage bias to the warming hiatus. *Geophys. Res. Lett.* **42**(7): 2385–2391, doi: 10.1002/2015GL063091.

Seneviratne SI, Corti T, Davin EL, Hirschi M, Jaeger EB, Lehner I, Orlowsky B, Teuling AJ. 2010. Investigating soil moisture – climate interactions in a changing climate: a review. *Earth Sci. Rev.* **99**(3–4): 125–161, doi: 10.1016/j.earscirev.2010.02.004.

Simmons AJ, Willett KM, Jones PD, Thorne PW, Dee DP. 2010. Low-frequency variations in surface atmospheric humidity, temperature, and precipitation: inferences from reanalyses and monthly gridded observational data sets. *J. Geophys. Res. Atmos.* **115**(D1): D01-110, doi: 10.1029/2009JD012442.

Skaugen T, Stranden H, Saloranta T. 2012. Trends in snow water equivalent in Norway (1931–2009). *Hydrol. Res.* **43**: 489–499, doi: 10.2166/nh.2012.109.

Sneyers R. 1990. On the statistical analysis of series of observations. WMO Technical Note, vol. 143, Secretariat of the World, Meteorological Organization, ISBN 9789263104151. www.wmo.int/pages/prog/wcp/agm/publications/technical_notes.php (accessed 14 June 2015).

Stahl K, Tallaksen LM, Hannaford J, van Lanen HAJ. 2012. Filling the white space on maps of European runoff trends: estimates from a multi-model ensemble. *Hydrol. Earth Syst. Sci.* **16**(7): 2035–2047, doi: 10.5194/hess-16-2035-2012.

Theil H. 1950. A rank-invariant method of linear and polynomial regression analysis. *Indag. Math.* **12**: 85–91. http://www.dwc.knaw.nl/DL/publications/PU00018789.pdf (accessed 17 March 2015).

Vautard R, Yiou P. 2009. Control of recent European surface climate change by atmospheric flow. *Geophys. Res. Lett.* **36**(22): L22-702, doi: 10.1029/2009GL040480.

Vikhamar-Schuler D, Hanssen-Bauer I. 2010. Long-term climate trends of Finmarksvidda, Northern-Norway. Technical Report met.no Report 06/2010 Climate, Norwegian Meteorological Institute, Oslo. http://met.no/Forskning/Publikasjoner/MET_report/2010/filestore/Ealat_climaterep_dvs.pdf (accessed 16 February 2016).

Vrac M, Vaittinada Ayar P, Yiou P. 2014. Trends and variability of seasonal weather regimes. *Int. J. Climatol.* **34**(2): 472–480, doi: 10.1002/jpc.3700.

Wapler K, James P. 2015. Thunderstorm occurrence and characteristics in Central Europe under different synoptic conditions. *Atmos. Res.* **158–159**: 231–244, doi: 10.1016/j.atmosres.2014.07.011.

Weedon GP, Balsamo G, Bellouin N, Gomes S, Best MJ, Viterbo P. 2014. The WFDEI meteorological forcing data set: WATCH forcing data methodology applied to ERA-Interim reanalysis data. *Water Resour. Res.* **50**(9): 7505–7514, doi: 10.1002/2014WR015638.

Werner PC, Gerstengarbe FW. 2010. Katalog der Grosswetterlagen Europas (1881–2009) nach Paul Hess und Helmut Brezowsky, 7th edn. Technical Report PIK Report 119, Potsdam Institute for Climate Impact Research (PIK), Potsdam, Germany. https://www.pik-potsdam.de/research/publications/pikreports/.files/pr119.pdf (accessed 2 April 2016).

Wilson D, Hisdal H, Lawrence D. 2010. Has streamflow changed in the Nordic countries? – recent trends and comparisons to hydrological projections. *J. Hydrol.* **394**(3–4): 334–346, doi: 10.1016/j.jhydrol.2010.09.010.

Yarnal B. 1993. *Synoptic Climatology in Environmental Analysis: A Primer*. Belhaven Press: London.

Zampieri M, D'Andrea F, Vautard R, Ciais P, de Noblet-Ducoudré N, Yiou P. 2009. Hot European summers and the role of soil moisture in the propagation of Mediterranean drought. *J. Clim.* **22**(18): 4747–4758, doi: 10.1175/2009jcli2568.1.

© 2016 Royal Meteorological Society